Biomolecular Detection and Quantification 15 (2018) 6–12

Contents lists available at ScienceDirect

Biomolecular Detection and Quantification

journal homepage: www.elsevier.com/locate/bdq

Research paper

An optimized targeted Next-Generation Sequencing approach for sensitive detection of single nucleotide variants

S. Stasik[a,c,1], C. Schuster[b,1], C. Ortlepp[b], U. Platzbecker[a], M. Bornhäuser[a,c], J. Schetelig[a], G. Ehninger[a], G. Folprecht[a,1], C. Thiede[a,*,1]

[a] Universitätsklinikum Carl Gustav Carus, Medizinische Klinik und Poliklinik I, Dresden, Germany
[b] AgenDix GmbH, Dresden, Germany
[c] National Center for Tumor Diseases (NCT), Heidelberg, Partner Site Dresden, Germany

ARTICLE INFO

Handled by Jim Huggett

Keywords:
Cancer
Minimal residual disease
Next-Generation sequencing
Low-level single nucleotide variants
Detection
Quantification

ABSTRACT

Monitoring of minimal residual disease (MRD) has become an important clinical aspect for early relapse detection during follow-up care after cancer treatment. Still, the sensitive detection of single base pair point mutations via Next-Generation Sequencing (NGS) is hampered mainly due to high substitution error rates. We evaluated the use of NGS for the detection of low-level variants on an Ion Torrent PGM system. As a model case we used the c.1849G > T (p.Val617Phe) mutation of the *JAK2*-gene. Several reaction parameters (e.g. choice of DNA-polymerase) were evaluated and a comprehensive analysis of substitution errors was performed. Using optimized conditions, we reliably detected *JAK2* c.1849G > T VAFs in the range of 0.01–0.0015% which, in combination with results obtained from clinical data, validated the feasibility of NGS-based MRD detection. Particularly, PCR-induced transitions (mainly G > A and C > T) were the major source of error, which could be significantly reduced by the application of proofreading enzymes. The integration of NGS results for several common point mutations in various oncogenes (i.e. *IDH1* and *2*, c-*KIT*, *DNMT3A*, *NRAS*, *KRAS*, *BRAF*) revealed that the prevalent transition vs. transversion bias (3.57:1) has an impact on site-specific detection limits of low-level mutations. These results may help to select suitable markers for MRD detection and to identify individual cut-offs for detection and quantification.

1. Introduction

The implementation of Next-Generation Sequencing (NGS) technologies into clinical diagnostics and research is a promising approach for the optimization of diagnosis and treatment of cancer. Malignant diseases are characterized by a stepwise and clonal accumulation of DNA sequence alterations that affect various cell signaling pathways, ultimately causing tumor initiation and progression [1]. Numerous genes are involved, among which several are affected in a variety of neoplasms (e.g. *KRAS*, *TP53*), whereas others are involved only in selected tumor entities (e.g. *IDH1*, *IDH2* in CNS tumors and leukemia) or even in specific diseases (e.g. *NPM1* mutations in myeloid leukemias) [2–5].

Detailed knowledge on the cancer genome and somatic hotspot mutations is crucial to improve risk assessment, to identify target lesions for specific treatment and to predict the response to therapy [6]. In addition to prognosis, molecular profiling is suitable to understand clonal evolution in cancer and to integrate adequate clinical biomarkers for the determination of minimal residual disease (MRD) status during long-term follow-up [7,8].

Based on a continuous decrease in costs and increase in throughput during the past years, NGS increasingly becomes an application for routine clinical testing [9]. While Sanger sequencing is largely restricted to a limited range of well-described mutations at specific genomic loci, the throughput of NGS enables novel diagnostic procedures using highly multiplexed mutational profiling across a large number of genes for virtually all types of DNA alterations [9,10] In addition to genome wide analyses, targeted NGS using amplicon resequencing allows the detection of point mutations with much higher sensitivity compared to Sanger sequencing. Accordingly, by increasing the number of reads per amplicon up to several 100000, it is theoretically possible to detect subclonal mutations at ultra-deep frequencies [11–13].

However, still there is paucity in the transfer and validation of NGS-

* Corresponding author: Universitätsklinikum Carl Gustav Carus, Medizinische Klinik und Poliklinik I, Fetscherstraße 74, 01307 Dresden, Germany.
E-mail address: christian.thiede@uniklinikum-dresden.de (C. Thiede).
[1] Equally contributing authors.

https://doi.org/10.1016/j.bdq.2017.12.001
Received 25 August 2017; Received in revised form 27 November 2017; Accepted 18 December 2017
Available online 09 January 2018

based MRD detection for routine clinical services, as sensitivity in massively parallel sequencing is typically limited due to high per-base substitution error rates (e.g. as a result of errors induced by DNA-polymerase) and by the capacity of NGS to process larger amounts of nucleic acids (template DNA input), typically needed for MRD detection [14]. Moreover, the specificity for low-frequency variants might vary across different target regions (e.g. various genes; high/low GC content sequences), enrichment technologies (e.g. hybridization capture and PCR amplicon based), tumor specimens and biopsy types, respectively [15,16].

In order to meet clinical standards and to distinguish true variants from sequencing errors, NGS has to be accurate and robust [17]. Several solutions have been described, e.g. the use of complex barcoding strategies, which enable the separation of true single nucleotide variants (SNVs) from errors [11–14]. Other procedures focused on minimizing false-positive variant calls at the respective genomic positions [18,19].

To further improve NGS based detection of SNVs we used an Ion Torrent PGM semiconductor system, which is well suited for targeted sequencing in clinical settings due to a comparably short running time and high accuracy for SNP calling [20]. As a model for optimization, we used the c.1849G > T mutation of the *JAK2*-gene leading to p.Val617Phe as a prototypical single base pair point mutation. In order to come up with an optimized procedure for the sensitive and quantitative application of NGS-based minimal residual disease detection, we carefully tested several reaction parameters to determine potential sources of error (e.g. the choice of an adequate proofreading polymerase, the amount of genomic template DNA, the number of PCR cycles etc.). We evaluated the reproducibility of our protocol on several other common target oncogenes (*IDH1* and *2*, c-*KIT*, *DNMT3A*, *NRAS*, *KRAS*, *BRAF*) which are potentially relevant as clinical biomarkers. In order to better understand the principal mechanisms behind the observed differences, we performed a more detailed analysis of substitution errors and could clearly show that transition errors, especially artefactual G > A substitutions, are the most common alteration. These results may lead to a better selection of suitable markers for MRD detection.

2. Material and methods

2.1. Samples and DNA extraction

Genomic DNA from the HEL cell line (DSMZ No. ACC 11, DSMZ, Braunschweig, Germany) (*JAK2* – p.Val617Phe positive) [21] or *JAK2* mutant patient samples was diluted in genomic DNA from healthy donors to obtain c.1849G > T variant allele frequencies (VAFs) of 0.001–10%. Control DNA was derived from healthy individuals (< 50 years of age) and served to assess per-base substitution error rates. Unless otherwise specified, DNA was extracted using DNeasy blood mini kit (Qiagen, Hilden, Germany) and quantified with a Qubit 2.0 fluorometer (Life Technologies Life Technologies, Grand Island, NY, USA). All patient samples were obtained with written informed consent of the patients, all studies involving human primary material were performed after approval of the local ethical board of the University Hospital Dresden.

2.2. Primer design and PCR amplification

PCR to detect the c.1849G > T mutation of the *JAK2*-gene was performed on genomic DNA with various concentrations of template DNA input (50 ng and 250 ng) as well as different PCR cycle numbers (35 and 40 cycles) using proofreading and non-proofreading polymerases from different vendors (Table 1). Fusion PCR primer for the preparation of amplicon libraries were designed (Primer Premier 6; Premier Biosoft, Palo Alto, CA, USA) according to the manufacturer's recommendations (Fusion Method; Life Technologies), illustrated in Supplementary Fig. S1. Briefly, the Fusion PCR method uses oligonucleotides containing the Ion A (5′-CCATCTCATCCCTGCGTGTC TCCGACTCAG-3′) and truncated P1 (trP1) (5′-CCTCTCTATGGGCAGT CGGTGAT-3′) adapters linked to a gene specific part to generate amplicons with the required motifs for parallel sequencing during the PCR. For unidirectional sequencing only one forward (with A adapter (or trP1 adapter)) and one reverse primer (with trP1 adapter (or A adapter)) were used for PCR amplification. Primer sequences for *JAK2* (p.Val617Phe) were 5′-GAAGCAGCAAGTATGATGAGCAAGC-3′ (Forward) and 5′-CTGAGAAAGGCATTAGAAAGCCTGTAGT-3′ (Reverse), amplifying a 182 bp fragment. PCR primer sequences and specific PCR conditions of all other target regions (*IDH1* and *2*, c-*KIT*, *DNMT3A*, *NRAS*, *KRAS*, *BRAF*) are listed in Supplemental Table S1. All PCR reactions were performed on a GeneAmp PCR System 9700 (Applied Biosystems, Foster City, CA, USA).

2.3. Library preparation, sequencing and data analysis

The PCR reactions were purified using a two-round purification process with Agencourt AMPure XP Reagent (Beckman Coulter, Krefeld, Germany) and eluted in 30–50 µl ddH_2O. The barcoded PCR products were quantified with a Qubit 2.0 fluorometer (Life Technologies) using the Qubit dsDNA HS Assay (Life Technologies) and sequenced uni-directionally on an Ion Torrent PGM semiconductor-based device (Life Technologies), according to manufacturer's protocols with 18 MOhm water and argon gas to drive fluidics. Briefly, the pooled library was clonally amplified on Ion Sphere™ Particles (ISPs) in an emulsion PCR using the Ion PGM Hi-Q OT2 Kit (Life Technologies). Enrichment of positive Ion Spheres (ISPs) was achieved using DynaBeadsMyOne streptavidin C1 beads (Life Technologies). Quantification of recovered particles was performed using a Qubit 2.0 fluorometer (Life Technologies) and an Ion Sphere quality control kit (Life Technologies). PGM sequencing (Ion PGM Hi-Q Sequencing Kit; Life Technologies) was done using different semiconductor chips, with output of 6×10^5 reads (314 chip), 3×10^6 reads (316 chip) and 6×10^6 reads (318 chip). Raw read mapping was done using Torrent Suite Software version 3.2 or higher based on the TMAP (Torrent Mapping Alignment Program) Smith-Waterman alignment algorithm using default settings with alignment to the hg19 human reference genome from the UCSC Genome Browser (http://genome.ucsc.edu/). For data analysis, adapter trimming and alignment QC we used the Torrent Variant Caller (TVC, v.4.0) plugin with default settings (somatic low stringency), providing optimized pre-set parameters for low-frequency variants assessment with minimal false negative calls.

3. Results

3.1. Application of NGS for the sensitive and quantitative detection of JAK2 (p.Val617Phe)

While there was a small but non-significant difference in base-calling error for the simultaneous increase of input DNA and reduction of PCR cycles (Fig. 1a), the application of high accuracy proofreading polymerases (Phusion HSII and Q5 High Fidelity) significantly (~5fold) reduced median per-base substitution error rates and consequently increased NGS sensitivity towards the identification of the *JAK2* c.1849G > T (p.Val617Phe) variant at 0.1% VAF (Fig. 1e-f). For all tested polymerases, PCR induced transitions (mainly G > A and C > T) were the major source of error, with an average transition bias vs transversion bias ratio of 3.57:1 (Fig. 1 b). Most significantly, Q5 High Fidelity polymerase reduced both transition and transversion bias, mainly for T > C (25fold), T > A and G > C (11fold each) substitution errors (compared to Platinum*Taq*). Virtually no difference between non-/proofreading enzymes was observed for A > G (1.35fold), C > G (1.25fold) and T > G (0.95fold) errors. Comparing sensitivity at c.1849G > T (*JAK2*) (Fig. 1c), false-positive G > T background was significantly reduced when the Q5 High Fidelity polymerase was used

Table 1
DNA polymerases and PCR conditions.

Enzyme/Vendor	PCR Reaction		PCR Conditions		
Platinum® *Taq*	Platinum PCR SuperMix	1x	Activation	94 °C	3 min
Invitrogen	each Primer	0.1 µM	Cycles	40	
	template DNA	varies	Denature	94 °C	30 s
			Anneal	X °C	30 s
			Extend	68 °C	1 min/kb
			Holding	4 °C	∞
Ampli*Taq* Gold®	PCR Gold Buffer	1x	Activation	95 °C	10 min
Applied Biosystems	dNTPs	0.2 mM	Cycles	25–35	
	$MgCl_2$	1.5 mM	Denature	95 °C	15 s
	each Primer	0.2 µM	Anneal	X °C	30 s
	Ampli*Taq* Gold	1.25 U	Extend	72 °C	1 min/kb
	template DNA	varies	Holding	4 °C	∞
Phusion Hot Start II®	Phusion HF Buffer	1x	Activation	98 °C	30 s
ThermoScientific	dNTPs	0.2 mM	Cycles	25–35	
	each Primer	0.5 µM	Denature	98 °C	5–10 s
	Phusion Hot Start II	1.00 U	Anneal	X °C	10–30 s
	template DNA	varies	Extend	72 °C	15–30 s/kb
			Final extend	72 °C	5–10 min
			Holding	4 °C	∞
Q5® High-Fidelity	Q5 Reaction Buffer	1x	Activation	98 °C	30 s
New England Biolabs	dNTPs	0.2 mM	Cycles	25–35	
	each Primer	0.5 µM	Denature	98 °C	5–10 s
	Q5 High-Fidelity	1.00 U	Anneal	X °C	10–30 s
	template DNA	varies	Extend	72 °C	20–30 s/kb
			Final extend	72 °C	2 min
			Holding	4 °C	∞

for amplicon generation, achieving an average G > T background rate of 0.0003 ± 0.0005% (Ø reads = 162068; range = 5942–853067), which could be further reduced by increasing coverage (Fig. S2). Likewise, based on dilution series of gDNA from the HEL cell line (Fig. 1d) we reliably detected and quantified c.1849G > T mutant allele frequencies down to 0.0015% (7 mutant alleles out of 463287 reads), which corresponds to a maximum sensitivity of ~1/66000 alleles and ~1/33000 cells, respectively, for heterozygous mutations.

3.2. NGS sensitivity for relevant point mutations

In order to assess the sensitivity and more general applicability of our approach for the detection of SNVs at mutational hotspots in various cancer-related genes, false-positive rates were assessed for a series of relevant single base pair point mutations, using the Q5 High Fidelity proofreading enzyme with a DNA template input of 250 ng and 35–40 PCR cycles (Ø coverage = 64017–231237) (Table 2). Sensitivity (expressed as false-positive variant calls) was below 0.1% for all tested genes. Integrating site-specific differences for all targets (Fig. 2), NGS sensitivity for hotspot mutations obviously correlated with median error rates previously determined for specific nucleotide changes (Fig. 1 b; Q5). Accordingly, PCR-induced transitions (G > A and C > T) at e.g. *DNMT3A* (c.2645G > A; c.2644C > T), *IDH1* (c.395G > A; c.394C > T), *IDH2* (c.419G > A; c.515G > A), *NRAS* (c.35G > A; c.34G > A) and *KRAS* (c.35G > A) occurred with significantly ($p < 0.05$) higher frequencies (Ø0.015 ± 0.016%) compared to false-positive transversions at e.g. c-*KIT* (c.2446G > T; c.2447A > T; c.2466T > A), *JAK2* (c.1849G > T) or *NRAS* (c.37G > C) with an almost ten-fold lower average background error of 0.002 ± 0.002%.

3.3. Clinical applicability of NGS for minimal residual disease detection

To evaluate the application of NGS for MRD detection, 152 serial follow-up samples of 15 patients (6f/9m), median age 59 yrs (range 22–77 yrs) with *JAK2*-mutated (c.1849G > T) diseases (PMF n = 13; secondary AML n = 2) were retrospectively analyzed post allogeneic stem cell transplantation (SCT). Median molecular follow-up time post transplantation was 1237 days (range 52–2697 days). Based on our experience from the validation studies, the analysis of clinical samples was performed with a defined cut-off of 1/10000 cells(Fig. 3). A total of 1.97×10^7 reads were generated with a median coverage of 126000 reads per sample (range 73000–207000). Three patients with sufficient molecular sampling (at least within 6 months prior to relapse) developed clinical relapse (283, 1193 and 1292 days post Tx). In all three patients, a significant increase in *JAK2* (p.Val617Phe) mutant alleles was observed by NGS prior to clinical relapse (179, 897 and 116 days post Tx) with a median delta between clinical and molecular relapse of 203 day (179–296 days). All patients remaining below the predefined threshold of 0.01% mutant alleles (indicating deep molecular response) remained in clinical remission.

4. Discussion

The adequate resolution of low-frequency SNVs is essential both to improve treatment of cancer and to monitor minimal residual disease status during follow-up. However, typically NGS sensitivity is limited to variants at 0.1–1% mainly due to sequencing related background errors [23]. Although this might be sufficient for most diagnostic purposes, especially for the assessment of inherited mutations, standard NGS approaches are not applicable to detect subclonal mutations relevant for MRD diagnostics. In order to reliably distinguish true variants from sequencing-related errors at mutant allele frequencies of < 0.1% and to identify suitable markers for MRD detection, we optimized Ion Torrent PGM-based NGS for the detection of single base pair point mutations and performed a detailed analysis on the type and frequency of substitution errors related to site-specific differences.

As demonstrated by the detection of the *JAK2* p.Val617Phe variant, a substantial proportion of substitution error was introduced during the PCR amplification process. Consequently, the application of proofreading enzymes significantly increased NGS sensitivity by reducing false-positive variant calls at the respective genomic positions. The importance of suitable enzymes, i.e. proofreading DNA-polymerases (containing 3′ → 5′ exonuclease activity) for high-fidelity requirements like the amplification for high-throughput sequencing and rare

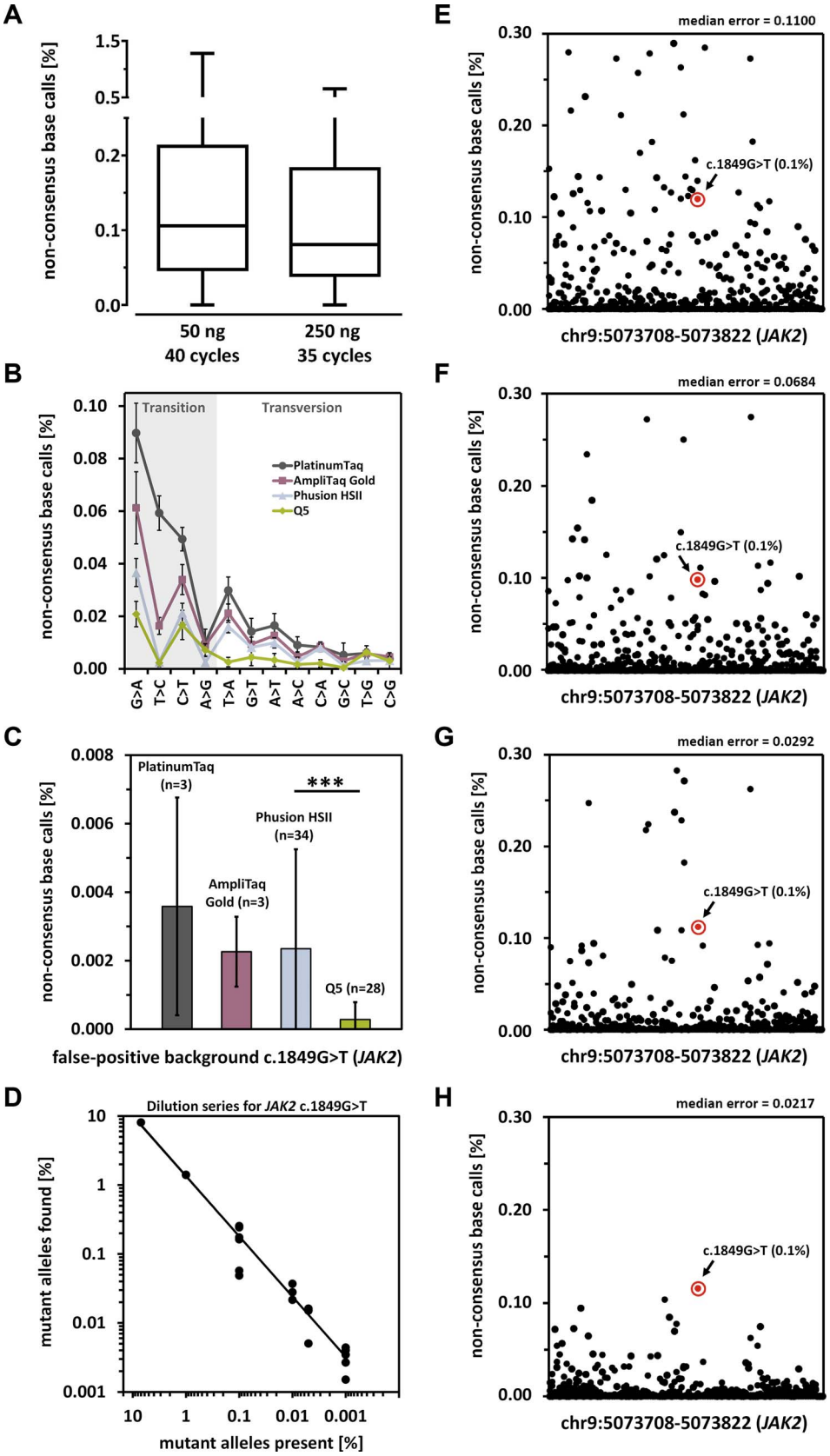

Fig. 1. Optimizing the application of NGS for the sensitive and quantitative detection of *JAK2* c.1849G > T (p.Val617Phe). **A:** Comparison of non-consensus base calls [%] (summing error rates of all 3 non-consensus bases for a particular nucleotide) for different amounts of genomic template DNA and PCR cycles using Platinum*Taq*. Data were calculated from triplicate measurements at chr9:5073708–5073822 (hg19) (*JAK2*) (Ø coverage = 236333). **B:** False-positive rates [%] for specific nucleotide substitutions. Data were calculated as median from triplicate measurements at chr9:5073708–5073822 (hg19) (*JAK2*) **C:** False-positive c.1849G > T (*JAK2*) background [%] from non-cancer human DNA. Data are shown for different non-proofreading and proofreading DNA-polymerases. Data were calculated as arithmetic mean ± standard deviation (Ø coverage = 162068). **D:** Serial dilution of DNA from the HEL cell line with a known mutation in *JAK2* c.1849G > T (p.Val617Phe) into non-cancer human DNA using Q5 polymerases. The coefficient of determination (r^2) between the prevalent mutant alleles and the VAF found with NGS was 0.9971 (Ø coverage = 176635; range = 53226–935957). **E–H:** Non-consensus base calls [%] of a *JAK2* p.Val617Phe positive control DNA, containing the c.1849G > T single base pair point mutation with a VAF of 0.1% (circled). Data are shown for four different DNA-polymerases: **E:** Platinum*Taq*, **F:** Ampli*Taq* Gold, **G:** Phusion HSII and **H:** Q5. Data were calculated as arithmetic mean of triplicate measurements at chr9:5073708–5073822 (hg19) (*JAK2*) (Ø coverage = 200442). Differences were analyzed using a two-tailed Student's *t*-test and a *p*-value of < 0.001*** was considered significant (shown as horizontal bar).

mutation detection, confirms previous reports [24,25]. Due to its particular relevance as the most frequent somatic change in myeloproliferative neoplasms [26], several assays (mainly qPCR-based) have already been described for the detection of *JAK2* p.Val617Phe with only some achieving a sufficient sensitivity for MRD detection [27–32]. As demonstrated by dilution series of *JAK2*-positive mutant DNA, we reliably detected *JAK2* c.1849G > T VAFs in the range of 0.01–0.0015% indicating the feasibility of PGM-based targeted Next-Generation

Table 2
NGS sensitivity for the detection of relevant point mutations using Q5 polymerases.

Target (AA Change)	Position [hg19]	Nuc. Change	False-positive variant calls [%]*			
IDH1 (p.Arg132His)	chr2:209113112	C > T (c.395G > A)	0.0079	±	0.0033	(n = 9; covØ133980)
IDH1 (p.Arg132Cys)	chr2:209113113	G > A (c.394C > T)	0.0070	±	0.0035	(n = 9; covØ134048)
IDH2 (p.Arg140Gln)	chr15:90631934	C > T (c.419G > A)	0.0043	±	0.0025	(n = 11; covØ231237)
IDH2 (p.Arg172Lys)	chr15:90631838	C > T (c.515G > A)	0.0069	±	0.0012	(n = 4; covØ108351)
JAK2 (p.Val617Phe)	chr9:5073770	G > T (c.1849G > T)	0.0003	±	0.0005	(n = 28; covØ162068)
c-*KIT* (p.Asp816Tyr)	chr4:55599320	G > T (c.2446G > T)	0.0020	±	0.0023	(n = 11; covØ90223)
c-*KIT* (p.Asp816His)	chr4:55599320	G > C (c.2446G > C)	0.0007	±	0.0023	(n = 11; covØ90223)
c-*KIT* (p.Asp816Val)	chr4:55599321	A > T (c.2447A > T)	0.0012	±	0.0014	(n = 12; covØ87332)
c-*KIT* (p.Asn822Lys)	chr4:55599340	T > G (c.2466T > G)	0.0048	±	0.0025	(n = 10; covØ106428)
c-*KIT* (p.Asn822Lys)	chr4:55599340	T > A (c.2466T > A)	0.0003	±	0.0006	(n = 10; covØ106428)
DNMT3A (p.Arg882His)	chr2:25457242	C > T (c.2645G > A)	0.0347	±	0.0313	(n = 7; covØ105193)
DNMT3A (p.Arg882Pro)	chr2:25457242	C > G (c.2645G > C)	0.0028	±	0.0030	(n = 7; covØ105193)
DNMT3A (p.Arg882Cys)	chr2:25457243	G > A (c.2644C > T)	0.0144	±	0.0216	(n = 7; covØ105241)
NRAS (p.Gly13Asp)	chr1:115258744	C > T (c.38G > A)	0.0082	±	0.0066	(n = 4; covØ109563)
NRAS (p.Gly13Arg)	chr1:115258745	C > G (c.37G > C)	0.0001	±	0.0002	(n = 4; covØ109599)
NRAS (p.Gly12Asp)	chr1:115258747	C > T (c.35G > A)	0.0454	±	0.0423	(n = 11; covØ96304)
NRAS (p.Gly12Ser)	chr1:115258748	C > T (c.34G > A)	0.0404	±	0.0099	(n = 11; covØ96345)
KRAS (p.Gly13Asp)	chr12:25398281	C > T (c.38G > A)	0.0028	±	0.0017	(n = 9; covØ97697)
KRAS (p.Gly12Val)	chr12:25398284	C > A (c.35G > T)	0.0068	±	0.0031	(n = 9; covØ84880)
KRAS (p.Gly12Asp)	chr12:25398284	C > T (c.35G > A)	0.0035	±	0.0026	(n = 9; covØ84880)
BRAF (p.Val600Glu)	chr7:140453136	A > T (c.1799T > A)	0.0048	±	0.0059	(n = 8; covØ64017)

* False-positive variant calls are presented as mean ± standard deviation. Number of replicate measurements (n) and mean coverage (covØ) are shown in parentheses. Targets were amplified using Q5 polymerase with amplification thermocycle consisting of: 98 °C for 30 s, followed by 35–40 cycles at 98 °C for 5 s, XX°C (see Table S1 for detailed information on annealing temperatures) for 10 s, and 72 °C for 20 s, final extension at 72 °C for 2 min.

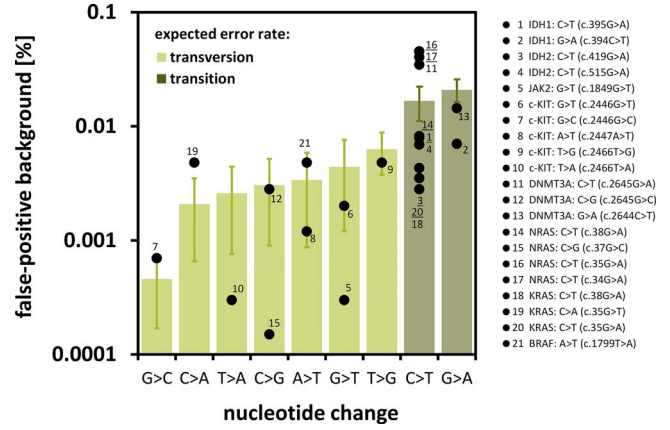

Fig. 2. Comparing median false-positive rates [%] for specific nucleotide substitutions (bars) with false-positive variant calls [%] determined at distinct mutational hotspots (dots) using Q5 polymerase and 250 ng of template DNA (Ø coverage = 64017–231237) (see also Table 2). Median false-positive rates for specific nucleotide substitution (bars) are based on the data presented in Fig. 1 b (Q5) and were calculated from triplicate measurements at chr9:5073708–5073822 (hg19) (*JAK2*) (Ø coverage = 215667).

Sequencing for the sensitive and quantitative detection of MRD using optimized conditions. These observations could be further validated by the retrospective analysis of clinical samples from patients after SCT, where a significant increase of *JAK2* (p.Val617Phe) mutant alleles was associated with subsequent relapse and occurred substantially earlier than the clinical relapse (179–296 days). Based on a mean G > T false-positive background of 0.0003% determined for the c.1849G > T substitution of the *JAK2*-gene, the theoretical detection limit for the p.Val617Phe variant would even correspond to 1/333333 alleles. However, assuming that 1 haploid human genome roughly contains 3 pg of DNA, this level of sensitivity can only by achieved with DNA template concentrations of > 1000 ng per PCR reaction. As we used a maximum of 250 ng of template DNA for amplification, the limit for quantitative detection was effectively restricted to 1 mutant-allele out of 83333 wt-alleles and 0.0012% (VAF), respectively. This sensitivity is in the range of false-positive rates (Ø = 0.0095%; range 0.0001–0.0454%) we determined for relevant point mutations and thus, in combination with sufficient sequencing depth (coverage), reasonable for most targets. Nevertheless, our approach would also be amenable for even higher concentrations of template DNA, which is in contrast to many other NGS-based approaches, where the maximum recommended DNA concentrations is 50 ng. Apart from the capacity to process larger amounts of template molecules, the final detection capability of a system is linked to the variances associated with the false-

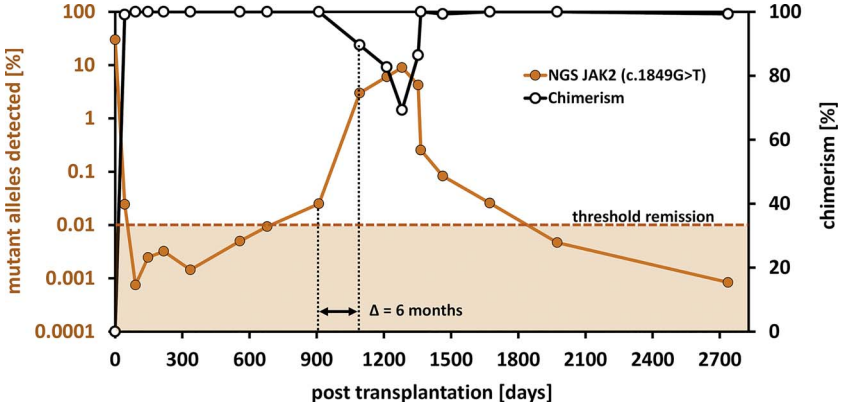

Fig. 3. NGS-based MRD detection in a patient with relapse after SCT using the c.1849G > T mutation of the *JAK2*-gene, Q5 polymerase and 5–250 ng of template DNA (median coverage 126000; range 73000–207000). The predefined threshold for molecular remission status is indicated at 0.01% VAF. Sequential analysis of chimerism in peripheral blood leukocytes was done using short tandem repeats (STR) PCR according to standard protocols [22].

positive rates [33]. According to this, a lower false-positive rate will automatically correlate with a lower abundance of a variant that can be measured significantly different from the background bias, which has to be considered in order to extrapolate final cut-offs for detection [33,34].

In line with previous findings [35,36], artefactual transitions (mainly G > A and C > T) were significantly over-represented compared to transversion bias (3.57:1), most likely due to molecular mechanisms including tautomeric shifts and/or spontaneous oxidative deamination [37]. As demonstrated by the integration of detection limits for various hotspot mutations, the difference in frequency of transition bias vs. transversion bias will lead to site-specific differences for the detection of low-level variants, ultimately affecting cut-offs for quantification and consequently the suitability of distinct SNVs as clinical markers for MRD monitoring. Hence, comparing specific sensitivity for relevant point mutations at *IDH1* and *2*, c-*KIT*, *DNMT3A*, *JAK2*, *NRAS*, *KRAS*, *BRAF*, transversion mutations may generally be better suited for early detection of residual disease via PCR amplicon-based NGS due to significant lower (~Ø10fold) false-positive rate relative to transition mutations. Interestingly, detection limits also partially varied within the same group of SNVs (e.g. up to one order of magnitude for C > T bias at *KRAS* p.Gly13Asp = 0.0028% and *NRAS* p.Gly12Asp = 0.0454%), indicating the presence of other factors (like DNA sequence-based motifs, inverted repeats and neighboring-nucleotide effects) [37,38] that determine the final source of substitution bias during amplification. Similarly, erroneous C > T transitions were found to be most pronounced when the subsequent base was a G in formalin-fixed, paraffin-embedded (FFPE) tumor specimens, indicating formalin-induced deamination of 5-methylcytosine at CpG dinucleotides [39].

Bias may also be introduced by DNA damage during prolonged temperature cycling, leading to substantial false-positives in amplification products [40]. Accordingly, the reduction of amplification cycles from 40 to 35 partially reduced artefactual background substitutions, most likely due to reduced non-enzymatic DNA damages and fewer nucleotide misincorporations by DNA polymerase. With respect to the detection of low-level SNVs, the reduction of PCR cycles and congruent increase of template DNA may also improve cut-offs for quantification by simultaneously reducing PCR artefacts and increasing prevalent mutant alleles. In addition to target enrichment and tissue specimens, platform specific bias (e.g. by inaccurate flow-calls) presumptively contributes to overall error, although PGM sequencing artefacts are relevant particularly for homopolymer-associated insertion/deletion (indel) errors (similar to 454 GS Junior; Roche Applied Science, Indianapolis, IN, USA) that account for the majority of bias introduced by PGM [41]. Moreover, recent reports on Ion Torrent sequencing artifacts also suggest that overall sequencing bias partially depends on the directionality of sequencing (using either universal forward plus a barcoded reverse primer or universal reverse plus a barcoded forward primer), indicating that DNA strand-specific bias and sequencing orientation may affect the detection of low-frequency substitutions during unidirectional sequencing [42]. According to this, the selection of forward vs. reverse strand sequencing may offer additional potential to systematically increase NGS sensitivity for distinct targets by specifically targeting less erroneous complementary substitutions at relevant sites of tumor associated point mutations. However, based on our experiences this might be appropriate particularly for non-proofreading enzymes that induced considerable differences in average background error for several complementary substitutions e.g. false-positives at T > C (~ 0.06%) vs. A > G (~ 0.01%) with Platinum*Taq* (Fig. 1b; Platinum*Taq*). Vice versa, only minor differences were observed for bias between most complementary substitutions when the proofreading polymerase Q5 was used (Fig. 1b; Q5), reducing the need to switch forward and reverse strand sequencing with optimized conditions.

As demonstrated in the present study, the optimization of Ion Torrent PGM-based Next-Generation Sequencing provides a practical approach for the targeted and quantitative detection of low-level single base pair point mutations in various oncogenes with sensitivities (false-positive variant calls) up to 10^{-4}. Recently, new approaches based on molecular tagging of single template molecules and subsequent error correction, were shown to further reduce NGS artifacts potentially enabling the detection of low-frequency variants among 10^{6}–10^{7} wild-type nucleotides [11,12]. However, application for clinical settings, particularly the compatibility with limited sample inputs and coverage of poorly captured sites, still needs to be assessed. We show that among several variables tested, the effects of PCR-based errors were most pronounced and that these artifacts can be avoided by the choice of an adequate proofreading enzyme for target amplification. This reduction of background substitutions significantly reduced false-positives and lead to an increased sensitivity. Results obtained from retrospective data (Fig. 3) further indicate that NGS-based MRD detection is clinically feasible and might provide a tool for early detection of relapse. Differences found in the frequency and type of PCR-induced substitution errors may help to predict NGS sensitivity at concrete mutational hotspots and accordingly has implications for the choice of accurate biomarkers. Since the principal mechanisms of amplification bias will be similar for all amplicon-based target enrichments, findings are also relevant and applicable to other Ion Torrent platforms (e.g. Ion S5). More importantly, our approach can be rapidly adopted for clinical purposes and serve as benchmark for future evaluations on the compatibility of Ion Torrent semiconductor-based NGS for the sensitive detection of low-frequency variants in different tumor specimens, like FFPE tissue or cell-free tumor DNA, relevant for clinical practice.

Funding

BMBF (Grant 031A424) and National Center for Tumor Diseases (NCT), Heidelberg, Partner Site Dresden, Germany.

Conflicts of interest

CT is CEO and co-owner of AgenDix GmbH, a company performing molecular diagnostics. SC and OC are employed at AgenDix GmbH. The remaining authors declare no conflict of interest.

Acknowledgments

For excellent technical assistance M Karger and M Hartwig are highly acknowledged. This study was supported in part by the German Federal Ministry of Research and Education (BMBF), Grant 031A424 “HaematoOPT” and by the National Center for Tumor Diseases (NCT) Heidelberg, Partner Site Dresden, Germany.

Appendix A. Supplementary data

Supplementary data associated with this article can be found, in the online version, at https://doi.org/10.1016/j.bdq.2017.12.001.

References

[1] M.R. Stratton, P.J. Campbell, P.A. Futreal, The cancer genome, Nature 458 (2009) 719–724.
[2] Y. Miki, J. Swensen, D. Shattuck-Eidens, P.A. Futreal, K. Harshman, S. Tavtigian, Q. Liu, C. Cochran, L.M. Bennett, W. Ding, et al., A strong candidate for the breast and ovarian cancer susceptibility gene *BRCA1*, Science (266) (1994) 66–71.
[3] H. Yan, D.W. Parsons, G. Jin, R. McLendon, B.A. Rasheed, W. Yuan, I. Kos, I. Batinic-Haberle, S. Jones, G.J. Riggins, H. Friedman, A. Friedman, D. Reardon, J. Herndon, K.W. Kinzler, V.E. Velculescu, B. Vogelstein, Bigner DD: *IDH1* and *IDH2* mutations in gliomas, N. Engl. J. Med. 360 (2009) 765–773.
[4] S. Eser, A. Schnieke, G. Schneider, D. Saur, Oncogenic KRAS signalling in pancreatic cancer, Brit. J. Cancer 111 (2014) 817–822.
[5] E. Papaemmanuil, M. Gerstung, L. Bullinger, V.I. Gaidzik, P. Paschka, N.D. Roberts, N.E. Potter, M. Heuser, F. Thol, N. Bolli, G. Gundem, P. Van Loo, I. Martincorena, P. Ganly, L. Mudie, S. McLaren, S. O'Meara, K. Raine, D.R. Jones, J.W. Teague, A.P. Butler, M.F. Greaves, A. Ganser, K. Döhner, R.F. Schlenk, H. Döhner,

P.J. Campbell, Genomic classification and prognosis in acute myeloid leukemia, N. Engl. J. Med. 374 (23) (2016) 2209–2221.
[6] J.P. Patel, M. Gönen, M.E. Figueroa, H. Fernandez, Z. Sun, J. Racevskis, P. Van Vlierberghe, I. Dolgalev, S. Thomas, O. Aminova, K. Huberman, J. Cheng, A. Viale, N.D. Socci, A. Heguy, A. Cherry, G. Vance, R.R. Higgins, R.P. Ketterling, R.E. Gallagher, M. Litzow, M.R. van den Brink, H.M. Lazarus, J.M. Rowe, S. Luger, A. Ferrando, E. Paietta, M.S. Tallman, A. Melnick, O. Abdel-Wahab, R.L. Levine, Prognostic relevance of integrated genetic profiling in acute myeloid leukemia, N. Engl. J. Med. 366 (2012) 1079–1089.
[7] M.J. Walter, D. Shen, L. Ding, J. Shao, D.C. Koboldt, K. Chen, D.E. Larson, M.D. McLellan, D. Dooling, R. Abbott, R. Fulton, V. Magrini, H. Schmidt, J. Kalicki-Veizer, M. O'Laughlin, X. Fan, M. Grillot, S. Witowski, S. Heath, J.L. Frater, W. Eades, M. Tomasson, P. Westervelt, J.F. DiPersio, D.C. Link, E.R. Mardis, T.J. Ley, R.K. Wilson, T.A. Graubert, Clonal architecture of secondary acute myeloid leukemia, N. Engl. J. Med. 366 (2012) 1090–1098.
[8] A. Ivey, R.K. Hills, M.A. Simpson, J.V. Jovanovic, A. Gilkes, A. Grech, Y. Patel, N. Bhudia, H. Farah, J. Mason, K. Wall, S. Akiki, M. Griffiths, E. Solomon, F. McCaughan, D.C. Linch, R.E. Gale, P. Vyas, S.D. Freeman, N. Russell, A.K. Burnett, D. Grimwade, Assessment of minimal residual disease in standard-Risk AML, N. Engl. J. Med. 374 (5) (2016) 422–433.
[9] M.L. Metzker, Sequencing technologies: the next generation, Nat. Rev. Genet. 11 (2010) 31–46.
[10] E.W. Klee, N.L. Hoppman-Chaney, M.J. Ferber, Expanding DNA diagnostic panel testing: is more better? Expert Rev. Mol. Diagn. 11 (2011) 703–709.
[11] S.R. Kennedy, M.W. Schmitt, E.J. Fox, B.F. Kohrn, J.J. Salk, E.H. Ahn, M.J. Prindle, K.J. Kuong, J.C. Shen, R.A. Risques, L.A. Loeb, Detecting ultralow-frequency mutations by duplex sequencing, Nat. Protoc. 9 (11) (2014) 2586–2606.
[12] J.B. Hiatt, C.C. Pritchard, S.J. Salipante, B.J. O'Roak, J. Shendure, Single molecule molecular inversion probes for targeted, high-accuracy detection of low-frequency variation, Genome Res. 23 (2013) 843–854.
[13] I. Kinde, J. Wu, N. Papadopoulos, K.W. Kinzler, B. Vogelstein, Detection and quantification of rare mutations with massively parallel sequencing, Proc. Natl. Acad. Sci. U. S. A. 108 (2011) 9530–9535.
[14] Q. Peng, R.V. Satya, M. Lewis, P. Randad, Y. Wang, Reducing amplification artifacts in high multiplex amplicon sequencing by using molecular barcodes, BMC Genom. 16 (2015) 589.
[15] A.G. Hadd, J. Houghton, A. Choudhary, S. Sah, L. Chen, A.C. Marko, T. Sanford, K. Buddavarapu, J. Krosting, L. Garmire, D. Wylie, R. Shinde, S. Beaudenon, E.K. Alexander, E. Mambo, A.T. Adai, G.J. Latham, Targeted, high-depth, next-generation sequencing of cancer genes in formalin-fixed, paraffin-embedded and fine-needle aspiration tumor specimens, J. Mol. Diagn. 15 (2) (2013 Mar) 234–247.
[16] D. Summerer, Enabling technologies of genomic-scale sequence enrichment for targeted high-throughput sequencing, Genomics 94 (2009) 363–368.
[17] C.J. Mattocks, M.A. Morris, G. Matthijs, E. Swinnen, A. Corveleyn, E. Dequeker, C.R. Müller, V. Pratt, A. Wallace, A standardized framework for the validation and verification of clinical molecular genetic tests, Eur. J. Hum. Genet. 18 (2010) 1276–1288.
[18] N. Pécuchet, Y. Rozenholc, E. Zonta, D. Pietraz, A. Didelot, P. Combe, L. Gibault, J.B. Bachet, V. Taly, E. Fabre, H. Blons, P. Laurent-Puig, Analysis of base-position error rate of next-generation sequencing to detect tumor mutations in circulating DNA, Clin. Chem. 62 (2016) 1492–1503.
[19] L. Worrillow, P. Baskaran, M.A. Care, A. Varghese, T. Munir, P.A. Evans, S.J. O'Connor, A. Rawstron, L. Hazelwood, R.M. Tooze, P. Hillmen, D.J. Newton, An ultra-deep sequencing strategy to detect sub-clonal TP53 mutations in presentation chronic lymphocytic leukaemia cases using multiple polymerases, Oncogene 35 (2016) 5328–5336.
[20] M.A. Quail, M. Smith, P. Coupland, T.D. Otto, S.R. Harris, T.R. Connor, A. Bertoni, H.P. Swerdlow, Y. Gu, A tale of three next generation sequencing platforms: comparison of ion torrent, pacific biosciences and Illumina sequencers, BMC Genom. 13 (2012) 341–354.
[21] H. Quentmeier, R.A. MacLeod, M. Zaborski, H.G. Drexle, JAK2 V617F tyrosine kinase mutation in cell lines derived from myeloproliferative disorders, Leukemia 20 (2006) 471–476.
[22] C. Thiede, M. Bornhauser, U. Oelschlagel, C. Brendel, R. Leo, H. Daxberger, B. Mohr, M. Florek, F. Kroschinsky, G. Geissler, R. Naumann, M. Ritter, G. Prange-Krex, T. Lion, A. Neubauer, G. Ehninger, Sequential monitoring of chimerism and detection of minimal residual disease after allogeneic blood stem cell transplantation (BSCT) using multiplex PCR amplification of short tandem repeat-markers, Leukemia 15 (2001) 293–302.
[23] T.C. Glenn, Field guide to next-generation DNA sequencers, Mol. Ecol. Resour. 11 (2011) 759–769.
[24] V. Marx, PCR: the price of infidelity, Nat. Methods 13 (2016) 475–479.
[25] A. Goldstein, P.V. Toro, J. Lee, J.L. Silberstein, M. Nakazawa, I. Waters, K. Cravero, D. Chu, R.L. Cochran, M. Kim, D. Shinn, S. Torquato, R.M. Hughes, A. Pallavajjala, M.A. Carducci, C.J. Paller, S.R. Denmeade, B. Kressel, B.J. Trock, M.A. Eisenberger, E.S. Antonarakis, B.H. Park, P.J. Hurley, Detection fidelity of AR mutations in plasma derived cell-free DNA, Oncotarget 8 (2017) 15651–15662.
[26] A. Tefferi, Molecular drug targets in myeloproliferative neoplasms: mutant ABL1JAK2MPLKITPDGFRAPDGFRB and FGFR1, J. Cell. Mol. Med. 13 (2) (2009) 215–237.
[27] J. Poodt, R. Fijnheer, I.B.B. Walsh, M.H.A. Hermans, A sensitive and reliable semi-quantitative real-time PCR assay to detect *JAK2* V617F in blood, Hematol. Oncol. 24 (2006) 227–233.
[28] N. Kroger, A. Badbaran, E. Holler, J. Hahn, G. Kobbe, M. Bornhauser, A. Reiter, T. Zabelina, A.R. Zander, B. Fehse, Monitoring of the JAK2-V617F mutation by highly sensitive quantitative real-time PCR after allogeneic stem cell transplantation in patients with myelofibrosis, Blood 109 (2007) 1316–1321.
[29] B. Denys, H. El Housni, F. Nollet, B. Verhasselt, J. Philippe, A real-time polymerase chain reaction assay for rapid, sensitive, and specific quantification of the *JAK2* V617F mutation using a locked nucleic acid-modified oligonucleotide, J. Mol. Diagn. 12 (2010) 512–519.
[30] U. Siebolts, T. Lange, D. Niederwieser, C. Wickenhauser, Allele-specific wild-type blocker quantitative PCR for highly sensitive detection of rare *JAK2* p.V617F point mutation in primary myelofibrosis as an appropriate tool for the monitoring of molecular remission following therapy, J. Clin. Pathol. 63 (2010) 370–372.
[31] G.V. Zapparoli, R.N. Jorissen, C.A. Hewitt, M. McBean, D.A. Westerman, A. Dobrovic, Quantitative threefold allele-specific PCR (QuanTAS-PCR) for highly sensitive *JAK2* V617F mutant allele detection, BMC Cancer 13 (2013) 206.
[32] M. Waterhouse, M. Follo, D. Pfeifer, N. von Bubnoff, J. Duyster, H. Bertz, J. Finke, Sensitive and accurate quantification of *JAK2* V617F mutation in chronic myeloproliferative neoplasms by droplet digital PCR, Ann. Hematol. 95 (5) (2016) 739–744.
[33] A.S. Whale, C. Bushell, P.R. Grant, S. Cowen, I. Guttierrez-Aguirre, D.M. O'Sullivan, J. Zel, M. Milavec, C.A. Foy, E. Nastouli, J.A. Garson, J.F. Huggett, Detection of rare drug resistance mutations by digital PCR in a human influenza A virus model system and clinical samples, J. Clin. Microbiol. 54 (2016) 392–400.
[34] C.A. Milbury, Q. Zhong, L. Lin, M. Williams, J. Olson, D.R. Link, B. Hutchison, Determining lower limits of detection of digital PCR assays for cancer-related gene mutations, Biomol. Detect. Quantif. 1 (1) (2014) 8–22.
[35] J. Brodin, M. Mild, C. Hedskog, E. Sherwood, T. Leitner, B. Andersson, J. Albert, PCR-induced transitions are the major source of error in cleaned ultra-deep pyrosequencing data, PLoS One 8 (7) (2013) e70388.
[36] M.S. Hestand, J.V. Houdt, F. Cristofoli, J.R. Vermeesch, Polymerase specific error rates and profiles identified by single molecule sequencing, Mutat. Res.-Fund Mol. M. 784 (-785) (2016) 39–45.
[37] Z. Zhao, E. Boerwinkle, Neighboring-nucleotide effects on single nucleotide polymorphisms: a study of 2.6 million polymorphisms across the human genome, Genome Res. 12 (11) (2002) 1679–1686.
[38] K. Nakamura, T. Oshima, T. Morimoto, S. Ikeda, H. Yoshikawa, Y. Shiwa, S. Ishikawa, M.C. Linak, A. Hirai, H. Takahashi, M. Altaf-Ul-Amin, N. Ogasawara, S. Kanaya, Sequence-specific error profile of Illumina sequencers, Nucleic Acids Res. 39 (13) (2011) e90.
[39] D.H. Spencer, J.K. Sehn, H.J. Abel, M.A. Watson, J.D. Pfeifer, E.J. Duncavage, Comparison of clinical targeted next-generation sequence data from formalin-fixed and fresh-frozen tissue specimens, J. Mol. Diagn. 15 (2013) 623–633.
[40] V. Potapov, J.L. Ong, Examining sources of error in PCR by single-molecule sequencing, PLoS One 12 (1) (2017) e0169774.
[41] L.M. Bragg, G. Stone, M.K. Butler, P. Hugenholtz, G.W. Tyson, Shining a light on dark sequencing: characterising errors in Ion Torrent PGM data, PLoS Comput. Biol. 9 (4) (2013) e1003031.
[42] S.J. Salipante, T. Kawashima, C. Rosenthal, D.R. Hoogestraat, L.A. Cummings, D.J. Sengupta, T.T. Harkins, B.T. Cookson, N.G. Hoffman, Performance comparison of Illumina and ion torrent next-generation sequencing platforms for 16S rRNA-based bacterial community profiling, Appl. Environ. Microbiol. 80 (24) (2014) 7583–7591.